Multi-field TDiff theories for cosmology

Diego Tessainer Bonet
Supervisors
Antonio López Maroto and María del Prado Martín Moruno.
Departamento de Física Teórica & IPARCOS, Universidad Complutense de Madrid.

We consider theories which break the invariance under diffeomorphisms (Diff) down to transverse diffeomorphisms (TDiff) in the matter sector, consisting of multiple scalar fields. In particular, we study models with two TDiff scalar fields in a flat Robertson-Walker spacetime and use the perfect fluid approach to study their dynamics. As a consequence of breaking the Diff symmetry, an effective interaction between the fields is induced from the conservation of the total energy-momentum tensor, which yields geometrical constraints different to those in single-field models. Thereupon, we introduce an application of these models concerning an interacting dark sector, and compare the theoretical predictions of our model to observations and wCDM.

I. INTRODUCTION

It is widely known, as observational data indicate, that our universe exhibits an accelerated expansion [1]. Many models explain this as the consequence of the domination of a dark energy component, taken to be a cosmological constant in the standard model, with there existing other alternatives, such as *quintessence*, involving a canonical scalar field with a dynamical equation of state [2]; and *k-essence* theories [3], which present non-canonical kinetic terms. Additionally, observations also indicate that most of the matter composition of our universe is dark matter [4]. There also exists a tension in the Hubble parameter H_0 measurement, which could be alleviated by models involving dark sector interactions or *phantom crossing*[5]. However, the nature of the dark sector is unknown. A way to address this problem is to consider possibe modifications of gravity on cosmological scales. With regards to this, multiple modified gravity theories extending upon General Relativity (GR) have been explored [6].

Even if GR provides a very powerful tool for studying gravity and cosmology, theories breaking invariance under diffeomorphisms (Diff) have been recently gaining popularity, with one of the most prominent ones being Unimodular Gravity (UG) [7]. In UG, the metric determinant is taken to be a fixed non-dynamical field and the Diff invariance is broken down to transverse diffeomorphisms (TDiff) and Weyl rescalings. UG theories have been capable of solving the vacuum-energy problem [8], although in this work we will focus on theories that are only invariant under TDiff, which have lately started to be studied more deeply. For instance, theories with a broken Diff invariance only in the Hilbert-Einstein action have been studied in [9], and TDiff invariant single-scalar field theories with broken symmetry in the matter sector have been explored in [10–12], presenting interesting phenomenology in cosmological backgrounds.

In this work we will consider multi-scalar TDiff invariant models in a flat Robertson-Walker (RW) spacetime in the matter sector. These fields present different coupling functions of the metric determinant in their potential and kinetic terms, which now need not be the canonical $\sqrt{g}$ [13]. We will mainly explore the kinetic domination regime and adopt the perfect fluid approach. The energy-momentum tensor (EMT) conservation will provide geometrical constrains different to those in the single-field case, and it will entail an effective interaction between the fields as a consequence of the symmetry breaking. We will study the single-field domination regimes and the energy exchange during these interactions, together with the analysis of the wide phenomenological variety provided by these models. Particularly, we will apply this model to describe an interacting dark sector, comparing its predictions with observations.

The work is organized as follows. In section II we briefly review the TDiff formalism and lay the groundwork for our particular models. Section III is devoted to explain the theoretical framework for multi-scalar TDiff models. In section IV we perform a numerical analysis for our model, applying it to the dark sector. Results will be compared both with observations and wCDM, and physical predictions for our TDiff model will be obtained. Finally, in section V we will discuss the conclusions.

II. SINGLE-FIELD TDIFF THEORIES

In this section we will present our model and briefly recap the main results obtained for TDiff theories involving one scalar field in the kinetic domination regime.

A. Transverse diffeomorphisms and matter action

Let us first consider a general infinitesimal coordinate transformation $x^\mu \mapsto x'^\mu = x^\mu + \xi^\mu(x)$ given by the vector field ξ. As we know, the metric tensor $(g_{\mu\nu}(x))$ variation will be given by its Lie derivative, i.e.,

$$\delta g_{\mu\nu} = \mathfrak{L}_\xi(g_{\mu\nu}) = -\nabla_\nu \xi_\mu - \nabla_\mu \xi_\nu, \tag{1}$$

and thus it follows that the metric determinant ($g := |\det(g_{\mu\nu})|$) will transform according to

$$\delta g = g g^{\mu\nu}\delta g_{\mu\nu} = -2g\nabla_\mu \xi^\mu. \tag{2}$$

Let us now write down our action. This is

$$S = S_{\rm HE}[g_{\mu\nu}] + S_{\rm mat}[g_{\mu\nu}, \phi_j], \tag{3}$$

where $S_{\rm mat}$ denotes the matter part of the action and ϕ_j denote the respective scalar fields we will consider. Since we will only break the Diff symmetry in the matter action, the geometrical part will just be the usual Hilbert-Einstein action

$$S_{\rm HE}[g_{\mu\nu}] = -\frac{1}{16\pi G}\int {\rm d}^4x\sqrt{g}R. \tag{4}$$

On the other hand, the matter part will read

$$S_{\rm mat}[g_{\mu\nu}, \phi_j] = \int {\rm d}^4x f(g)\mathcal{L}(g_{\mu\nu}(x), \phi_j(x), \partial_\mu\phi_j(x)), \tag{5}$$

where $\mathcal{L}$ denotes the corresponding scalar under Diff Lagrangian density and $f(g)$ an arbitrary function of the metric determinant. Recalling (1) and (2) we can compute $\delta_\xi S$, which, after integration by parts and assuming that the fields vanish at infinity, reads [10]

$$\delta_\xi S = \int {\rm d}^4x\partial_\mu\xi^\mu(f(g) - 2gf'(g))\mathcal{L}. \tag{6}$$

Thus, we see that the action is invariant under Diff only when $f(g) - 2gf'(g) = 0$, i.e. $f(g) \propto \sqrt{g}$. However, the action still preserves a smaller subgroup of symmetry, corresponding to transformations satisfying $\partial_\mu\xi^\mu = 0$, which correspond to transverse diffeomorphisms.

B. Single scalar field models in the kinetic regime

Before we present our dark sector model, we will briefly recap the main results obtained for the single-scalar field model in a cosmological background. Let us first write the matter part of the action [10, 11]:

$$S_{\rm mat} = \int {\rm d}^4x\left(\frac{1}{2}f_{\rm K}(g)\partial_\mu\phi\partial^\mu\phi - f_{\rm V}(g)V(\phi)\right), \tag{7}$$

where $V(\phi)$ denotes the potential and $f_{\rm K}$, $f_{\rm V}$ are positive functions of the metric determinant. On the other hand, since we are not modifying the Hilbert-Einstein action, the Bianchi identities are preserved and thus the local conservation of the EMT and Einstein equations will still hold [10, 11]. The EMT will be defined as usual:

$$T^{\mu\nu} := -\frac{2}{\sqrt{g}}\frac{\delta S_{\rm mat}}{\delta g_{\mu\nu}}, \tag{8}$$

which in this case reads

$$T_{\mu\nu} = \frac{f_{\rm K}(g)}{\sqrt{g}}\left(\partial_\mu\phi\partial_\nu\phi - F_{\rm K}g_{\mu\nu}\Box\phi\right) + 2\frac{f_{\rm V}(g)}{\sqrt{g}}F_{\rm V}g_{\mu\nu}V(\phi), \tag{9}$$

where we have defined $F_i := {\rm d}\ln f_i(g)/{\rm d}\ln g$, $i = {\rm K}, {\rm V}$.

In relation to the background geometry, we will consider a spatially flat FLRW metric. Since we have less symmetry than in the Diff case, we will not generally be able to perform a coordinate change that fixes the time component g_{00} to one. This is a result of having less gauge freedom than in GR, which follows from the transversality condition [14]. Thus, our spacetime will be described by the following metric:

$$ds^2 = b^2(\tau){\rm d}\tau^2 - a^2(\tau)\mathbf{dx}^2, \tag{10}$$

where $a(\tau)$ and $b(\tau)$ are the independent components that will act as the scale factor and shift function, respectively. Both must be computed from Einstein equations. Particularly, the equation for the G^{00} component of the Einstein tensor yields [14]

$$\left(\frac{a'}{a}\right)^2 = \frac{8\pi G}{3}\rho b^2, \tag{11}$$

which is the usual Friedmann equation in time τ. Notice that it recovers its original shape under the coordinate transformation ${\rm d}t = b(\tau){\rm d}\tau$, where t will be referred to as *cosmological time*. We will denote $' = {\rm d}/{\rm d}\tau$ and $\cdot = {\rm d}/{\rm d}t$.

Let us now apply the perfect fluid approach. It is worth recalling that, when $\partial_\mu\phi$ is a time-like vector, the EMT takes the form [11]

$$T_{\mu\nu} = (\rho + p)u_\mu u_\nu - pg_{\mu\nu}, \tag{12}$$

where $\rho = T^0_0$ denotes the energy density, $p = -1/3T^i_j\delta^j_i$ is the pressure, and u_μ is the four-velocity of the fluid, a time-like vector. Recalling (9) and using (10) we get

$$\rho = \frac{f_{\rm K}(g)}{b^2\sqrt{g}}\left(1 - F_{\rm K}\right)(\phi')^2 + 2\frac{f_{\rm V}(g)}{\sqrt{g}}F_{\rm V}V(\phi), \tag{13}$$

$$p = \frac{f_{\rm K}(g)}{b^2\sqrt{g}}F_{\rm K}(\phi')^2 - 2\frac{f_{\rm V}(g)}{\sqrt{g}}F_{\rm V}V(\phi); \tag{14}$$

where we assumed for simplicity the case of a homogeneous field $\phi = \phi(\tau)$. Before we recap the physical results for the kinetic domination regime, let us write the equations of motion of $\phi(\tau)$ in this spacetime using the Euler-Lagrange equations [10]:

$$\phi''(\tau) + \phi'(\tau)\frac{L'(\tau)}{L(\tau)} + b^2\frac{f_{\rm V}(g)}{f_{\rm K}(g)}\frac{{\rm d}V}{{\rm d}\phi} = 0, \tag{15}$$

where $L(\tau) := f_{\rm K}(g(\tau))/b^2(\tau)$. Lastly, the zeroth component of the EMT conservation equation $\nabla_\nu T^{\mu\nu} = 0$ yields the following useful result [10]:

$$\rho' + 3\frac{a'}{a}(\rho + p) = 0. \tag{16}$$

We will study the kinetic domination regime (for further analysis on the potential case see [10, 11]). In this case,

by neglecting the potential contributions in (13) and (14) it is straightforward to see that $p = w_\phi \rho$, where

$$w_\phi := \frac{p}{\rho} = \frac{F_{\rm K}(g)}{1 - F_{\rm K}(g)}; \tag{17}$$

which will generally depend on τ and, thus, the equation of state parameter w_ϕ will evolve throughout time. One particular case takes place when the coupling function is a power-law, i.e., $f_{\rm K}(g) = kg^\alpha$, where k and α are constants. In this case we obtain for w_ϕ:

$$w_\phi = \frac{\alpha}{1-\alpha} = \text{const.} \tag{18}$$

Notice how this requires $\alpha < 1$ in order for the weak energy condition to be satisfied [11]. The equation of motion (15) in this limit implies that $\phi'(\tau) = C_\phi / L(\tau)$, with $C_\phi = $ const.. Substituting this in equations (13), (14); factoring out $\rho + p$ in (16) and recalling $g = b^2 a^6$ the conservation law (16) reads

$$\frac{\rm d}{{\rm d}\tau} \ln\!\left(a^6\right) = g'(\tau) \frac{\rm d}{{\rm d}g} \left[\ln\left((1 - 2F_{\rm K}(g)) \frac{g}{f_{\rm K}(g)} \right) \right], \tag{19}$$

which provides the geometrical constraint that allows the conservation law (16) to be satisfied. This is [10]:

$$\frac{g}{f_{\rm K}(g)} \left(1 - 2F_{\rm K}(g)\right) = C_g a^6. \tag{20}$$

This geometrical constrain on g allows us to obtain the relation between b and a for any given coupling. For instance, if $f_{\rm K}(g) \propto g^\alpha$ (20) implies that $b \propto a^{3\alpha/(1-\alpha)}$. Notice that if we take $\alpha = 1/2$ (Diff limit) we obtain that in the kinetic regime $\rho(a) \propto a^{-6}$, which depicts the behavior of a stiff fluid; a fluid whose equation of state is $p = \rho$. Some of the models used to explain stiff fluids use what are called *kination fields*, these being scalar fields dominated by their kinetic terms, and can be found in some inflationary contexts [15, 16]. In conclusion, the TDiff formalism enables a much wider phenomenology for kinetically driven fields, as opposed to the Diff case in which we are limited to stiff fluids.

III. MULTI-FIELD TDIFF MODELS

In this section we will present our new approach, consisting of two TDiff homogeneous scalar fields in the matter action with different coupling functions, both in the kinetic regime. Our action will read

$$S_{\rm mat} = \int {\rm d}^4x \sum_{i=1}^{2} \left(\frac{1}{2} f_{{\rm K}_i}(g) \partial_\mu \phi_i \partial^\mu \phi_i \right). \tag{21}$$

Notice that we did not consider an interaction potential between both fields. As we will see, the energy exchange and the rich phenomenology will arise from geometrical constrains coming from the conservation of the total EMT, since the individual EMTs of each field will not be conserved as a consequence of the symmetry breaking.

The individual energy density and pressure of each field will therefore be given by (13) and (14), neglecting the respective potential term contributions. We will also consider power-law coupling functions, i.e., $f_{{\rm K}_1} = kg^\alpha$, $f_{{\rm K}_2} = \lambda g^\beta$. Recalling the equation of motion (15), we can see that $\phi_i'(\tau) = C_{\phi_i}/L_i(\tau)$. Substituting these into the respective pressures and energy densities, recalling the conservation equation (16) and proceeding analogously to the one field case we get the geometrical constrain

$$C_{\phi_1}^2 \frac{g|2F_{{\rm K}_1} - 1|}{f_{{\rm K}_1}} + C_{\phi_2}^2 \frac{g|2F_{{\rm K}_2} - 1|}{f_{{\rm K}_2}} = C_g a^6, \tag{22}$$

which in the power-law coupling case yields

$$C_1 g^{1-\alpha} |2\alpha - 1| + C_2 g^{1-\beta} |2\beta - 1| = C_g a^6; \tag{23}$$

where $C_1 = C_{\phi_1}^2/k$ and $C_2 = C_{\phi_2}^2/\lambda$. This is a very illuminating result, since as we observe from (23) it does not require the individual EMT conservation of each field and thus it will involve a geometrical-like interaction between the two components caused by the symmetry breaking. However, this equation is complicated to solve and we might need a numerical treatment.

Lastly, here we include the expression for the energy density in the power-law coupling case, which will be of valuable use throughout the rest of the work:

$$\rho(a,b)_i = C_i(1-\alpha_i) \frac{b^{1-2\alpha_i}}{a^{6\alpha_i+3}}, \tag{24}$$

which is obtained from (13) neglecting the potential term.

A. Approximate results: single-field domination

Let us first consider the general case in which one of the fields, for example ϕ_1, dominates over the other, ϕ_2. We can thus neglect the contribution of ϕ_2 in (23), so

$$C_1 g^{1-\alpha} |2\alpha - 1| \simeq C_g a^6 \Rightarrow b \propto a^{3w_1}, \tag{25}$$

where $w_1 = \alpha/(1-\alpha)$ and $w_2 = \beta/(1-\beta)$. This is the same geometrical constrain one would obtain if ϕ_1 was the only field. Notice that this is just an approximation that provides the leading order of $b(a)$, but it gives us valuable information concerning the evolution of the energy densities in the different domination regimes. In terms of the conservation equations, this translates into

$$\rho_1' + 3\frac{a'}{a}(\rho_1 + p_1) = Q = -\rho_2' - 3\frac{a'}{a}(\rho_2 + p_2), \tag{26}$$

$$0 = \rho_1' + 3\frac{a'}{a}(\rho_1 + p_1) + \rho_2' + 3\frac{a'}{a}(\rho_2 + p_2) \simeq \rho_1' + 3\frac{a'}{a}(\rho_1 + p_1); \tag{27}$$

where Q is commonly referred to as the *interacting kernel* in the literature [17]. Recalling (24) and using (19) yields

$$\rho_1(a) \propto a^{-3(1+w_1)} \quad , \quad \rho_2(a) \propto a^{-3(1+w_{\text{eff}})}; \tag{28}$$

and thus ϕ_1 decays as expected from its equation of state, but ϕ_2 will exhibit a decay as if it were a perfect fluid with constant equation of state parameter $w_{\text{eff}} \neq w_2$, where

$$w_{\text{eff}} = \frac{2w_2 - w_1 + w_1 w_2}{1 + w_2}. \tag{29}$$

This was obtained by replacing the geometrical constrain (25) in ρ_2 and equating to $Ca^{-3(1+w_{\text{eff}})}$. Fig.1 summarizes the wide range of possible phenomenology for the subdominant component.

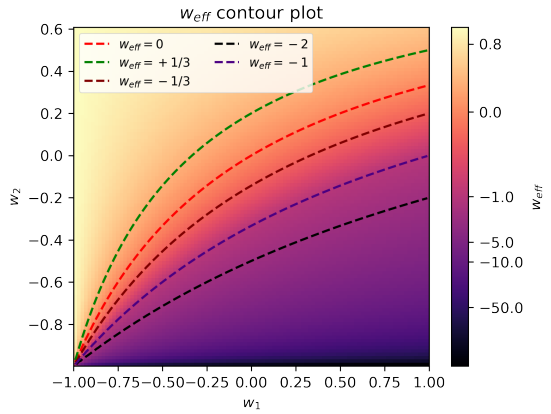

FIG. 1. w_{eff} of ϕ_2 under ϕ_1 domination.

This result happens to be physically illuminating with regards to cosmological contexts. As we can see above, interactions between perfect TDiff fluids with different equation of state parameters allow for a wide range of possible evolutions for the subdominant component. In particular, as the above dotted lines indicate, all of the possible dark energy behaviors are plausible for the subdominant field, including phantom dark energy [18] ($w_{\text{eff}} < -1$, its energy density increases over time) and *quintessence*. We emphasize that these behaviors have been obtained without the addition of non-canonical kinetic terms [3], they are a result of breaking the Diff symmetry. Interestingly, although $w_i < -1$ is not allowed for each individual field, the dominance regimes allow for subdominant phantom behavior without violating the energy conditions. As a result, this provides a vast range of possibilities to describe an interacting dark matter-dark energy sector ($w_1 = 0$, $w_2 < -1/3$) with an evolving dark energy given by a function $w_{\text{eff}}(a)$ stemming from the broken Diff invariance, exhibiting phantom decay at early times during the matter epoch.

B. Energy exchange

We will now analyze the exchange of energy between the fields induced by the effective interaction, and its evolution through the several field domination regimes by studying the interacting kernel Q. Let us consider two scalar fields ϕ_1 and ϕ_2 in the kinetic regime, with equation of state parameters w_1 and w_2. Let us also assume that ϕ_1 dominates over ϕ_2. Recalling (29) and (24), using the conservation law (16) in the domination approximation yields the following expression:

$$Q = 3C_2(1-\beta)\frac{a'}{a}a^{-3(1+w_{\text{eff}})(w_{\text{eff}}-w_2)}. \tag{30}$$

Using (24) and writing both conservation equations in terms of ρ_1 and ρ_2, respectively,

$$\rho_1' + 3\frac{a'}{a}(\rho_1 + p_1) = 3\rho_2\mathcal{H}\frac{-w_2^2 + w_2 - w_1 + w_1 w_2}{1 + w_2}, \tag{31}$$

$$\rho_2' + 3\frac{a'}{a}(\rho_2 + p_2) = -3C_2\mathcal{H}(1-\beta)(w_{\text{eff}} - w_2)\left(\frac{\hat{C}_1}{\rho_1}\right)^{\zeta(w_1,w_2)}; \tag{32}$$

where we defined $\hat{C}_1 \equiv 1 - \alpha$, $\zeta(w_1, w_2) = (-3w_2 + w_1 - w_1 w_2 - 1)/(1 + w_2 + w_1 + w_1 w_2)$ and $\mathcal{H} = a'/a$ denotes the Hubble parameter in time coordinate τ.

We will now study the sign of Q during this domination regime. Firstly, we observe from (31) that Q has two zeros, those being at $w_{\text{eff}} = w_2$, i.e., $w_2 = w_1$ and $w_2 = 1$. The analysis in the ϕ_2 domination regime is fully akin to the previous one, but we have to perform the change $w_1 \mapsto w_2$ and change the sign of Q (remember we defined Q with respect to the conservation law for ϕ_1). We distinguish three cases: $w_1, w_2 < 1$, $w_1, w_2 > 1$, $w_1 > 1, w_2 < 1$. However, the last two involve components that are beyond stiff fluids ($w_i > 1$), and thus are not particularly interesting for our dark sector model. We will hence focus on the first one from now on. We get, for $w_1, w_2 < 1$, the results in Tab.I:

$w_2 \in I_1$	$w_2 \in I_2$
$Q < 0$	$Q > 0$
$w_1 \in I_1'$	$w_1 \in I_2'$
$Q > 0$	$Q < 0$

TABLE I. Flux of energy: ϕ_1 domination regime, depending on w_2 for $w_1 < 1$ (subtable 1); ϕ_2 domination regime depending on w_1 for $w_2 < 1$ (subtable 2);

where $I_1 = (-1, w_1)$, $I_2 = (w_1, 1)$ and the I_i' are the same as their I_i partners but interchanging w_1 and w_2. We can hence observe that the direction of the energy flux will not change between both domination regimes. More clearly, if we assume $w_1 > w_2$ then when ϕ_1 dominates $Q < 0$ and ϕ_1 loses energy in favor of ϕ_2, with the same happening as well when ϕ_2 is dominant. The same reasoning can be applied for the case $w_1 < w_2$, allowing us to conclude that in this case it is the field with the greater w_i who always loses energy.

In terms of the dark sector, notice that in (31) $w_{\text{eff}} = -1/3$ when $w_2 = (-1 + 3w_1)/(7 + 3w_1) \equiv \mathcal{A} < w_1$.

This separates the region of w_2 values in which the subdominant field starts decaying as dark energy. Similarly, $w_{\rm eff} = -1$ occurs at $w_2 = (-1+w_1)/(3+w_1) \equiv \mathcal{B}$ and it corresponds to the phantom behavior boundary for ϕ_2. Hence, if $w_1 < 1$ we can see that if $w_2 \in (-1, \mathcal{B})$ the subdominant component will exhibit phantom dark energy behavior and the dominant field will lose energy in favor of this (see Tab.I); and if $w_2 \in (\mathcal{B}, \mathcal{A})$ it will also gain energy from the dominant component ϕ_1, but not enough to display phantom nature.

More specifically, if we consider a dark sector model consisting of dark matter (DM) with $w_1 = 0$ and dark energy (DE), with $w_2 < -1/3$, we can observe that DE will always be phantom during the matter domination epoch due to the energy flux from DM ($Q < 0$). The energy exchange will occur in the same direction when DE dominates, although it will now not be enough to keep the phantom behavior, and the DE decay will gradually transition to resemble its asymptotic value for the equation of state parameter w_2. On the other hand, DM will slowly start to exhibit a different decay than the typical a^{-3} as DE becomes more dominant, see (29).

C. Analytical model

Solving the general constrain (23) is not a simple task, and it usually requires numerical treatment. We will later do this for generic dark sector models with $w_1 = 0$ (DM) and $w_2 < -1/3$ (DE), so we can get theoretical predictions that can be compared to observations. However, there is a particular dark sector model for which (23) can be analytically solved, consisting of DM ($w_1 = 0, \alpha = 0$) and DE with $w_2 = -1/2, \beta = -1$. Despite not being the best fitting model, as we will later see, being analytical provides us with a wide insight to further understand TDiff models. The constrain (23) then reads

$$C_1 g + 3C_2 g^2 = C_g a^6, \tag{33}$$

which is quadratic in g. Thus, we get

$$g = -\frac{C_1}{6C_2} + \frac{\sqrt{C_1^2 + 12C_2C_g a^6}}{6C_2}; \tag{34}$$

which allows us to explicitly obtain the relation $b(a)$:

$$b(a) = \sqrt{\frac{C_1}{6C_2}} \left[a^{-6} \left(\sqrt{1 + \frac{12C_2C_g}{C_1^2} a^6} - 1 \right) \right]^{1/2}; \tag{35}$$

valid for all values of a. It is worth remarking that, in this model, during the respective DM and DE domination regimes the Friedmann equation (11) recovers its usual Diff form when the only fields are non-relativistic matter or DE, respectively, thus yielding an expanding universe. As we will later see, the faraway past $a \ll 1$ will correspond to the matter era, and in the future $a \gg 1$ DE will be dominant, as expected.

For $a \ll 1$, expanding (35) in powers of a yields

$$b(a)_{a\ll 1} \simeq \sqrt{C_g} C_1 \left(1 - \frac{3}{2} \frac{C_2 C_g}{C_1^2} a^6 \right), \tag{36}$$

from which we can obtain the respective energy densities:

$$\rho_1(a) \simeq \sqrt{C_1 C_g} [a^{-3} - 3C_2C_g/(2C_1^2) a^3], \tag{37}$$

$$\rho_2(a) \simeq 2(C_g/C_1)^{3/2} C_2 a^3. \tag{38}$$

Notice how the DM (ρ_1) decay is governed by the a^{-3} term, which corresponds to the expected behavior according to $w_1 = 0$. Consequently, DM is dominant at early times. Besides, DE (ρ_2) evolves with a^3, exhibiting the phantom nature we previously discussed (in particular, $w_{\rm eff} = -2$) as a result of it gaining energy from DM. This can be illustrated writing the conservation equations for each component in terms of the energy density of the other, which read:

$$\rho_1' + 3\frac{a'}{a}\rho_1 = -\frac{9}{2}\mathcal{H}\rho_2, \tag{39}$$

$$\rho_2' + 3\frac{a'}{a}(\rho_2 + p_2) = +9C_g^2 \frac{C_2}{C_1} \mathcal{H} \frac{1}{\rho_1}; \tag{40}$$

where the phantom nature is exposed in (40) as a result of ρ_1 appearing in the denominator.

On the other hand, for $a \gg 1$, expanding (35) yields

$$b(a)_{a\gg 1} \simeq \sqrt{\frac{C_1}{6C_2}} \left(\sqrt{A} a^{-3/2} - \frac{1}{\sqrt{2}A} a^{-9/2} \right), \tag{41}$$

with $A \equiv \sqrt{12C_2C_g/C_1^2}$. The energy densities thus read

$$\rho_1(a) = \frac{C_1^{3/2}}{\sqrt{6C_2}} \left(\sqrt{A} a^{-9/2} - \frac{1}{2\sqrt{A}} a^{-15/2} \right), \tag{42}$$

$$\rho_2(a) = \frac{C_1^{3/2}}{6^{3/2} C_2^{1/2}} (-3a^{-9/2}\sqrt{A} + 2a^{-3/2}A^{3/2}). \tag{43}$$

The leading order for great values of a in ρ_2 indicates that now our DE will decay as expected from its equation of state ($w_2 = -1/2$), and DM decays faster than a^{-3}. This implies that at later times it is DE who becomes dominant, and from the reasoning of the previous subsection, we can see that DM is still giving energy to DE, but not enough to keep the phantom behavior as DM starts becoming subdominant. One could write analogous expressions to (39) and (40), but they are not as physically enlightening due to the lack of phantom nature.

We will now write the exact expressions for both energy densities in order to discuss the whole evolution. From the previous analysis we know that both energy densities become equal at a certain time: $a = a_{\rm eq}$, $\rho_i = \rho_{\rm eq}$. We

can thus write ρ_1 and ρ_2 substituting (35) in (24) and equating them. We obtain

$$C_1 = \frac{5}{2}\rho_{\rm eq}^2 a_{\rm eq}^6 C_g^{-1} \quad , \quad C_2 = \frac{125}{16}\rho_{\rm eq}^4 a_{\rm eq}^6 \frac{1}{C_g^3}; \tag{44}$$

which yield

$$\rho_1(z) = \frac{1}{\sqrt{3}}\rho_{\rm eq}\left(\frac{1+z}{1+z_{\rm eq}}\right)^6 \sqrt{\Theta(z)}, \tag{45}$$

$$\rho_2(z) = \frac{1}{\sqrt{27}}\rho_{\rm eq}\left(\frac{1+z}{1+z_{\rm eq}}\right)^6 \sqrt{\Theta(z)^3}; \tag{46}$$

where we defined $\Theta(z) \equiv \sqrt{1+15((1+z_{\rm eq})/(1+z))^6} - 1$, and where $z = 1/a - 1$ denotes the redshift.

We will now obtain some physical results and compare this model to ΛCDM before plunging into the general case. Firstly, recalling (24) and the conservation law (16), we can parameterize the decay of each component with a function $w_{\rm eff,i}(z)$ which satisfies

$$\rho'_i + 3\frac{a'}{a}(1 + w_{\rm eff,i}(z))\rho_i = 0; \tag{47}$$

which yields the following result when recalling (24):

$$w_{\rm eff,i}(z) = -\frac{1}{3}\left(-\frac{1+z}{b(z)}(1-2\alpha_i)\frac{{\rm d}b}{{\rm d}z} - 6\alpha_i - 3\right) - 1. \tag{48}$$

This recovers the previously studied constant results when considering the respective field domination regimes. The functions $w_{\rm eff,i}$ can easily be simplified for the analytical case since we know $b(z)$. Using the exact expression for $b(z)$ (35) yields the result in Fig.2, for several values of the free parameter $z_{\rm eq}$. Notice how in reality we only have $z_{\rm eq}$ as our free parameter, since the condition $(\rho_1 + \rho_2)\big|_{t=t_0} = (1 - \Omega_{\rm B})\rho_{\rm c}$ must be satisfied and, thus, it enforces an extra relation between the parameters. As a reminder, $\Omega_{\rm B}$ depicts the baryonic matter component of the universe and $\rho_{\rm c}$ is the critical density.

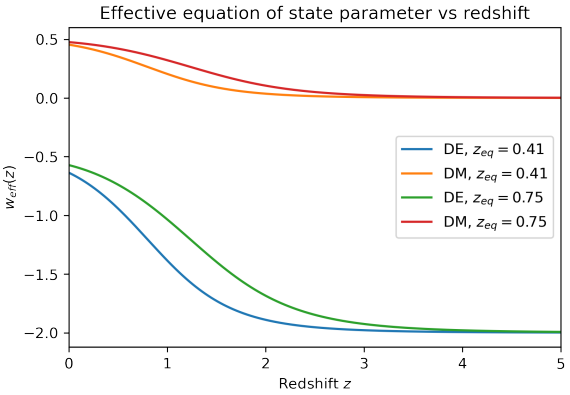

FIG. 2. $w_{\rm eff}(z)$ for DM and DE for various $z_{\rm eq}$.

In this work we assumed that only the dark sector breaks the Diff invariance, hence we will treat baryons as Diff matter. As we can see from Fig.2, the DE decay behavior starts being phantom-like at early times, as expected, and then evolves in time until it reaches the asymptotic value reflected in the equation of state $w_2 > -1$ in the future, with the parameter $z_{\rm eq}$ only changing the behavior in the intermediate regimes. On the other hand, DM will exhibit its usual a^{-3} decay at early times but it will decay faster when DE starts to dominate. In light of this we can see that TDiff models can provide very rich phenomenology involving a time evolving decay for the dark sector, as opposed to ΛCDM in which DM always decays with a^{-3} and DE is a cosmological constant. This could lead to innovative models with a cosmological-constant like DE today, but with $w \neq -1$ at early times.

Lastly, we will analyze this model from the perspective of the density parameters to further understand TDiff dark sector models. We will denote the density parameters for DM and DE, respectively, as $\Omega_{\rm DMT}$ and $\Omega_{\rm DET}$. We will also use the standard notation for the ΛCDM parameters: $\Omega_{\rm M} = \Omega_{\rm DM} + \Omega_{\rm B}$ for matter and Ω_Λ for the cosmological constant. Recalling the Friedmann equation (11) and using cosmological time ${\rm d}t = b(\tau){\rm d}\tau$ yields

$$H^2 = \frac{8\pi G}{3}(\rho_{\rm B} + \rho_1 + \rho_2). \tag{49}$$

Multiplying and dividing this expression by the Hubble parameter at $t = t_0$ (today) H_0^2, and recalling that $\rho_{\rm c} = 8\pi G/(3H_0^2)$ it is straightforward to obtain

$$\Omega_{\rm DMT}(z) = \frac{1}{\sqrt{3}}\frac{\rho_{\rm eq}}{\rho_{\rm c}}\left(\frac{1+z}{1+z_{\rm eq}}\right)^6 \frac{\sqrt{\Theta(z)}}{E^2(z)}, \tag{50}$$

$$\Omega_{\rm DET}(z) = \frac{1}{3\sqrt{3}}\frac{\rho_{\rm eq}}{\rho_{\rm c}}\left(\frac{1+z}{1+z_{\rm eq}}\right)^6 \frac{\sqrt{\Theta(z)^3}}{E^2(z)}, \tag{51}$$

where we defined

$$E^2(z) \equiv \Omega_{\rm B}(1+z)^3 + \frac{\rho_{\rm eq}}{\sqrt{3}\rho_{\rm c}}\left(\frac{1+z}{1+z_{\rm eq}}\right)^6 \sqrt{\Theta(z)}\left[1 + \frac{\Theta(z)}{3}\right]. \tag{52}$$

This allows us to obtain the time evolution for each density parameter. This will obviously depend on the specific value of $z_{\rm eq}$, but the general tendency will be similar. For the sake of simplicity, we included the case $z_{\rm eq} = 1.1$ in the Fig.3 to show qualitative results. This results in a higher DE density parameter and a lower DM density parameter at $t = t_0$ than those from ΛCDM, which can be interpreted as a consequence of the phantom era during the DM domination regime. As we previously discussed, DM grants DE a lot of energy, which translates into its phantom behavior and thus contributes to obtaining higher values of $\Omega_{\rm DET}$. It is worth mentioning, however, that we shall not compare these parameters to those from ΛCDM, as $\Omega_{\rm DMT}$ and $\Omega_{\rm DET}$ may not be regarded as *true* DM and DE density parameters, since,

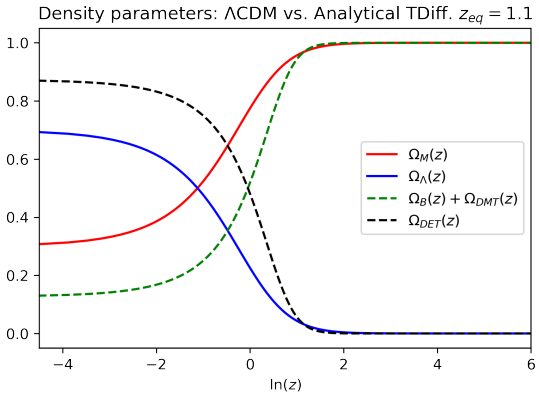

FIG. 3. Evolution of the density parameters: ΛCDM vs analytical TDiff case ($z_{\rm eq} = 1.10$).

as opposed to ΛCDM, this model presents an interacting dark sector and thus there may be contributions from both components to each parameter. Nonetheless, something that we could look out for in TDiff models is compatibility with the CMB measurement of $\Omega_{\rm M}$, since at the decoupling time ($z_{\rm dec} \simeq 1100$ [19]) the DE contribution is negligible and DM is approximately dominant.

IV. A TDIFF MODEL FOR DARK SECTOR INTERACTIONS

We will now consider a more general case with $w_1 = 0$, which could play the role of DM; and arbitrary $w_2 < -1/3$, which could play the role of DE. We will then contrast their predictions to observations. Recalling the geometrical constrain (23) arisen from the conservation of the EMT, using $\alpha = 0$ and dividing by C_2 yields

$$\frac{C_1}{C_2} g + g^{1-\beta} |2\beta - 1| = \frac{C_g}{C_2} a^6. \tag{53}$$

It may seem as if we had two other free parameters, those being the quotients of the several integration constants; but in reality there is only one. Without loss of generality, we can fix the gauge condition $a(t_0) = 1$, and also $g(t_0) = 1$, which leads to $b(t_0) = 1$. Notice how we can fix the second condition as well, since performing this change will be reflected in the action (21) as a global constant $\mathcal{C}$, $\tilde{S}_{\rm mat} = \mathcal{C} S_{\rm mat}$; both actions being physically equivalent under a redefinition of the fields embodying this change: $\phi_i \mapsto \tilde{\phi}_i = \sqrt{\mathcal{C}}\phi_i$. Thus, evaluating (53) at t_0 we get

$$\frac{C_1}{C_2} + |2\beta - 1| = \frac{C_g}{C_2} \equiv k. \tag{54}$$

It is also worth noticing that

$$\frac{\rho_1(t_0)}{\rho_2(t_0)} = \frac{C_1}{C_2}(1-\beta)^{-1} = \frac{\Omega_{\rm DMT}}{\Omega_{\rm DET}} \equiv \lambda. \tag{55}$$

Therefore, we only have two free parameters, those being the exponent of the power-law coupling function of the DE component, β and λ. However, we will use another physical parameter instead of λ in order to obtain a more direct analysis and an easier comparison to observations. In fact, recalling Friedman equation (49) in cosmological time, using (24) and noting that $(\rho_1 + \rho_2)\big|_{t_0} = (1-\Omega_{\rm B})\rho_{\rm c}$ yields the following expression for $H^2(z)$:

$$H^2 = H_0^2 \left[\Omega_{\rm B}(1+z)^3 + (1-\Omega_{\rm B}) \left(1 + \frac{1}{\lambda}\right)^{-1} b(z)(1+z)^3 \right. \\ \left. + (1-\Omega_{\rm B}) \frac{1}{\lambda} \left(1 + \frac{1}{\lambda}\right)^{-1} b(z)^{1-2\beta}(1+z)^{6\beta+3} \right], \tag{56}$$

where we neglected radiation, as the purpose of this model is to study the DM and DE domination epochs. Otherwise, we should have included the respective $\Omega_{\rm R}(1+z)^4$ contribution, assuming it is a Diff component. Thus, if we consider the decoupling time ($z_{\rm dec} \simeq 1100$), at which the DE contribution is negligible and most part of $\Omega_{\rm DMT}(z_{\rm dec})$ will come from DM, we will just have the respective matter and radiation components in $H^2(z)$. This allows us to define the following effective density parameter for total matter at high z:

$$\Omega_{\rm M}^{\rm eff} \equiv \Omega_{\rm B} + (1-\Omega_{\rm B}) \left(1 + \frac{1}{\lambda}\right)^{-1} b_{\rm early}, \tag{57}$$

which can be compared to the CMB measurement for $\Omega_{\rm M}$ [19]($\Omega_{\rm M} = 0.315 \pm 0.007$). $b_{\rm early}$ denotes the value of the shift function at high redshift, which is constant as matter dominates at high z (see (25)). We will use this parameter $\Omega_{\rm M}^{\rm eff}$ instead of λ, since both are trivially related through (57). Acknowledge that $b_{\rm early}$ can be directly computed from the conservation equation (53) taking into consideration that DM dominates at this time and radiation does not contribute to the geometrical constrain, since we are treating it as a Diff component and thus its EMT is automatically conserved because of the lack of any interaction terms in the action. Thus, recalling (25), using (54) and (55) yields:

$$b_{\rm early} = \sqrt{\frac{\lambda(1-\beta) + |2\beta - 1|}{\lambda(1-\beta)}}. \tag{58}$$

This will allow us to fit our parameters $(\beta, \Omega_{\rm M}^{\rm eff})$ to observations and obtain physical predictions for this model. In particular, we developed a code in *Python* that solves the conservation law (53) for any given pair of these two parameters. Hence, we can obtain $b(z)$ and $H(z)$ through (56). We will then regard the Union2-database observational data coming from type Ia Supernovae [20] consisting of 557 data for $0.015 < z < 1.030$ and compare them to the theoretical distance moduli $\mu(z)$ predictions of our model. We will study the agreement between theory and observations using the χ^2 statistical estimator [20]:

$$\chi^2 = \sum_i \frac{(\mu^{\rm obs}(z_i) - \mu^{\rm th}(z_i))^2}{E_i^2}, \tag{59}$$

where the theoretical distance modulus is given by

$$\mu^{\rm th}(z) = 5\log_{10}(H_0 d_{\rm L}(z)) + M = \hat{\mu}(z) + M, \qquad (60)$$

with M the absolute magnitude, which we marginalized:

$$M = \sum_i \left(\frac{1}{\sigma} \frac{\hat{\mu}(z_i) - \mu^{\rm obs}(z_i)}{E_i^2} \right). \qquad (61)$$

E_i denotes the error in the μ_i measurement at redshift z_i and $\sigma = \sum_i E_i^{-2}$. On the other hand, $d_{\rm L}(z)$ is the luminosity distance, computed from

$$d_{\rm L}(z) = (1+z)r(z) = (1+z)\chi(z) = (1+z)\int_0^z \frac{{\rm d}z}{H(z)}, \qquad (62)$$

where χ is the co-moving radial distance and r the radial coordinate, both being the same in this case since we are considering flat spatial hypersurfaces. Numerical integration will allow us to perform the analysis in the subsequent sections.

A. One-parameter fit

We will first start by studying which β value for the coupling exponent of the dark energy field fits best to the observational data, when fixing $\Omega_{\rm M}^{\rm eff}$ to the central value measured by Planck CMB observations [19]. This will allow us to get a glimpse of the viability of this model before tackling the two parameter case, in which we will regard $\Omega_{\rm M}^{\rm eff}$ as another free parameter (notice from (57) that fixing $\Omega_{\rm M}^{\rm eff}$ leaves us with β as our only free parameter). We considered a set of 400 values of β lying in the interval $(-30, -0.5)$ and computed the distance moduli using (60) for the respective redshift values present in Union2 data. This allows us to study the agreement between our models and observations by using the χ^2 estimator defined above. The model minimizing χ^2 will be the best fit to the observational data. For the sake of comparison, we will also include the results obtained from the respective wCDM fit, for which the distance moduli are computed from (60), the Hubble parameter being the only difference:

$$H(z)_{w{\rm CDM}} = H_0\sqrt{\Omega_{\rm M}(1+z)^3 + \Omega_\Lambda(1+z)^{3(1+w)}}, \qquad (63)$$

for the DM and DE domination eras, where w denotes the constant DE equation of state. This allows us to compare our one-parameter TDiff fit to the analogous wCDM fit when considering w as the only free parameter by fixing $\Omega_{\rm M}$ to the CMB measurement (we used 400 values of w in (-2,0)). This yields the result in Tab.II.

	Best fit	$\chi^2_{\rm min}$
TDiff	$\beta = -2.792$ ($w_2 = -0.736$)	543.28
wCDM	$w = -1.112$	542.73

TABLE II. One-parameter fit: TDiff vs wCDM results.

We can thus infer that both models provide excellent concordance to observations, with the minimal χ^2 differing just a 0.10% between them. As we know, in ΛCDM, dark energy is a cosmological constant with a non-dynamical equation of state. However, in our ideal TDiff model, it would be a TDiff component with $p = -0.736\rho$ but a dynamical decay behavior given by an effective parameter $w_{\rm eff}$, given through (48). Using (48) for the best TDiff fit allows us to obtain the DE decay behavior for all redshifts. Thus, the DE component would have been phantom in the past under DM domination and afterwards would slowly transition until reaching the asymptotic decay reflected by w_2 (quintessence dark energy). Numerically we obtained that $w_{\rm eff} \sim -0.80$ today, which indicates that our DE would be close to a cosmological constant at recent times. We also include the 1-σ region of the equation of state parameter w_2:

$$w_2 = -0.736^{+0.041}_{-0.005}. \qquad (64)$$

B. Two-parameter fit

We will lastly analyze our TDiff model without constraining $\Omega_{\rm M}^{\rm eff}$, which will allow us to conclude if the actual best TDiff fit is compatible with the CMB measurement for $\Omega_{\rm M}^{\rm eff}$, and, if not, how far it is from it. On the grounds of this, we will consider a set of 73 values for β in the interval $(-40, -0.5)$ and 73 values of $\Omega_{\rm M}^{\rm eff}$ in the interval $(0.15, 0.56)$. For each possible pair of values, we calculated the distance moduli using (60) and then computed the respective χ^2 estimator for each case with (59). In the following analysis we will also include the direct wCDM analogue of this two-parameter fit, in which both $\Omega_{\rm M}$ and w are fitted (using a 73×73 grid with $w \in (-2, 0)$ and $\Omega_{\rm M} \in (0.01, 0.60)$), in order to compare both models. Numerical analysis thus yields the results in Tab.III.

	Best fit	$\chi^2_{\rm min}$
TDiff	$\beta = -4.340$ ($w_2 = -0.813$), $\Omega_{\rm M}^{\rm eff} = 0.389$	542.16
wCDM	$w = -1.055$, $\Omega_{\rm M} = 0.289$	542.63

TABLE III. Two-parameter fit: TDiff vs wCDM.

These indicate that both models fit extremely well to observations, with TDiff even achieving this subtly better. Lastly, we focus on the TDiff case and present the contour plot for both parameters up to the 4-σ region in Fig.4, from which we can infer that, not only does our TDiff model provide excellent concordance with observational data, but it is also compatible with the $\Omega_{\rm M}$ CMB measurement in the 1-σ region.

We can also obtain the 1-σ intervals for each of the parameters by marginalizing the likelihood

$$\mathcal{L}(\beta, \Omega_{\rm M}^{\rm eff}) = \mathcal{N}{\rm e}^{-\chi^2/2}, \qquad (65)$$

which can be done for each variable by performing the

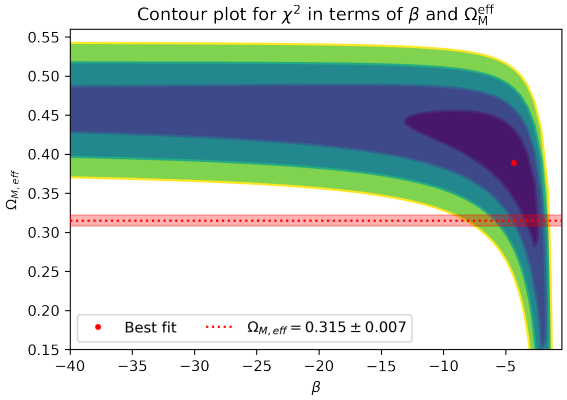

FIG. 4. Two-parameter fit: contour plot for χ^2 up to 4-σ.

integration with respect to the other. This yields:

$$\mathcal{L}^{\rm m}(\beta) = \mathcal{N}_1 \int {\rm e}^{-\chi^2/2} {\rm d}\Omega_{\rm M}^{\rm eff}, \quad \mathcal{L}^{\rm m}(\Omega_{\rm M}^{\rm eff}) = \mathcal{N}_2 \int {\rm e}^{-\chi^2/2} {\rm d}\beta; \tag{66}$$

where $\mathcal{N}_1$ and $\mathcal{N}_2$ are normalization constants. The maximization of these marginalized likelihood distributions $\mathcal{L}^{\rm m}$ allow us to obtain the following 1-σ regions for both of the parameters, which have been obtained from the GetDist package[1]:

$$\beta = -4.340^{+2.460}_{-9.981} \quad , \quad \Omega_{\rm M}^{\rm eff} = 0.390^{+0.083}_{-0.003}.$$

Notice how, as expected from Fig.4, the model's dependence on β is weaker than on $\Omega_{\rm M}^{\rm eff}$, with the latter being the more determinant parameter when comparing to observations. This is a consequence of the flexibility provided by two-field TDiff models, since, as we saw before, all the possible dark energy components transition from phantom at early times to standard DE behavior, and it is not the equation of state parameter w_2 which dictates the decay behavior until the distant future. Fig.5 summarizes the results of the best fitting model and its comparison to wCDM, displaying excellent agreement with observations, and also to wCDM, although there start being minor differences between both models at higher redshift values.

Lastly, we include the evolution of the effective equation of state parameter for the DE and DM components for the best fitting model in Fig.6. We see that today DE approximately behaves like a cosmological constant, as in ΛCDM (numerically, $w_{{\rm eff},2}(t_0) \sim -0.90$). As a result, TDiff models favor the presence of dynamical DE, starting from phantom at early times and slowly transitioning to usual quintessence DE, with an asymptotic quintessence decay dictated by w_2), roughly being a cosmological constant at current times. Similarly, DM will exhibit a faster decay than that expected from

[1] `https://getdist.readthedocs.io/`.

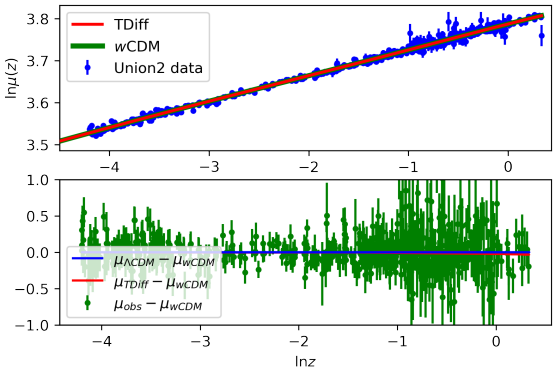

FIG. 5. Best fit: comparison to wCDM and observations.

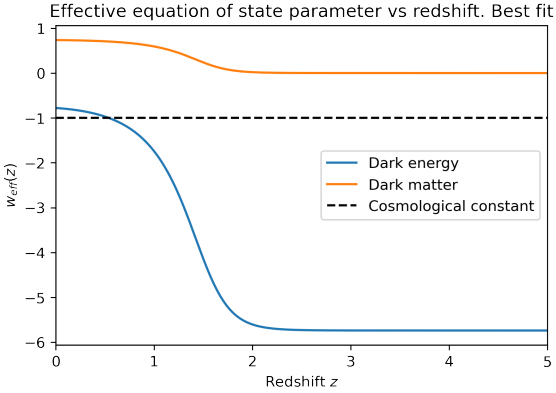

FIG. 6. $w_{\rm eff}(z)$ for the two-parameter best fit.

$w_1 = 0$ at recent times as a consequence of the symmetry breaking, without the usual a^{-3} decay being altered during the matter era. It is worth remarking that this time-evolving DE behavior involving phantom-constant-quintessence transitions was obtained without enforcing any type of interaction potential in the Lagrangian, and without the addition of non-canonical or *ghost* terms in the matter action.

V. CONCLUSIONS

In this work, we have considered theories with two scalar fields breaking the Diff symmetry down to TDiff and studied their cosmological consequences. We have focused on their kinetic domination regimes and analyzed the geometrical conditions imposed by the conservation of the total EMT, which still holds as a consequence of the Bianchi identities. When working in a flat FLRW background, this allows to obtain the g_{00} parameter, which is now physical as a consequence of the symmetry breaking.

This geometrical constraint enforces an exchange of energy between both fields, as their individual EMTs are not conserved. In light of this, we proposed a dark sector

model involving two TDiff scalar fields coupled to gravity through power-law functions, with one depicting dark matter and the other depicting dark energy. We regarded the different field domination regimes and showed that, although the equation of state parameters are constant, both components will exhibit a different dynamical decay as that corresponding to Diff models with the same parameters. Particularly, when imposing that DM decays as a^{-3} at early times we show that the DE component will present phantom behavior during the matter era, for it to slowly transition into usual DE behavior in the future. This interacting model for the dark sector is obtained without the need of non-canonical terms or any interacting potentials introduced by hand. We also studied the evolution of the energy exchange and showed how in these models it is always DE which gains energy from DM, and we also considered a particular analytical case to deeply understand the physics involved in these particular TDiff models.

Lastly, we studied this particular model deeply from a numerical perspective. We considered two parameters: β (the coupling exponent for the DE field, closely linked to its equation of state parameter) and $\Omega_{\rm M}^{\rm eff}$ (an effective density parameter at high redshift values, which can be easily compared to the CMB measurement for $\Omega_{\rm M}$). We used the Union2 data for Ia supernovae and fitted our two parameters to these observations, showing exceptional compatibility with them, and a goodness of the fit similar to that of wCDM. In addition, the best fitting region for our parameters at 1-σ is compatible with the CMB measurement of the matter density parameter; and DE, while exhibiting a dynamical behavior, would approximately be a cosmological constant today.

Notwithstanding the above, there is future work that can be done regarding these theories. Specifically, stability under cosmological perturbations should be profoundly investigated, in order to study structure formation from the TDiff perspective. The covariantized approach, studied in [21], could be of special relevance in this case. Other possible future approaches could involve the use of more general coupling functions or non-homogeneous fields, as well as breaking the symmetry in the Einstein-Hilbert action too and studying the potential and mixed regimes.

[1] A. G. R. et. al., Observational evidence from supernovae for an accelerating universe and a cosmological constant, The Astronomical Journal **116**, 1009 (1998).

[2] S. Tsujikawa, Quintessence: A Review, Class. Quant. Grav. **30**, 214003 (2013), arXiv:1304.1961 [gr-qc].

[3] C. Armendariz-Picon, V. F. Mukhanov, and P. J. Steinhardt, Essentials of k essence, Phys. Rev. D **63**, 103510 (2001), arXiv:astro-ph/0006373.

[4] K. Freese, Review of Observational Evidence for Dark Matter in the Universe and in upcoming searches for Dark Stars, EAS Publ. Ser. **36**, 113 (2009), arXiv:0812.4005 [astro-ph].

[5] E. Di Valentino, A. Mukherjee, and A. A. Sen, Dark Energy with Phantom Crossing and the H_0 Tension, Entropy **23**, 404 (2021), arXiv:2005.12587 [astro-ph.CO].

[6] T. Clifton, P. G. Ferreira, A. Padilla, and C. Skordis, Modified Gravity and Cosmology, Phys. Rept. **513**, 1 (2012), arXiv:1106.2476 [astro-ph.CO].

[7] R. Carballo-Rubio, L. J. Garay, and G. García-Moreno, Unimodular gravity vs general relativity: a status report, Class. Quant. Grav. **39**, 243001 (2022), arXiv:2207.08499 [gr-qc].

[8] G. Ellis, H. van Elst, J. Murugan, and J.-P. Uzan, On the trace-free einstein equations as a viable alternative to general relativity, Classical and Quantum Gravity **28**, 225007 (2011).

[9] A. G. Bello-Morales and A. L. Maroto, Cosmology in gravity models with broken diffeomorphisms, Phys. Rev. D **109**, 043506 (2024), arXiv:2308.00635 [gr-qc].

[10] A. L. Maroto, TDiff invariant field theories for cosmology, JCAP **04**, 037, arXiv:2301.05713 [gr-qc].

[11] D. Jaramillo-Garrido, A. L. Maroto, and P. Martín-Moruno, TDiff in the dark: gravity with a scalar field invariant under transverse diffeomorphisms, JHEP **03**, 084, arXiv:2307.14861 [gr-qc].

[12] D. Alonso-López, J. de Cruz Pérez, and A. L. Maroto, Unified transverse diffeomorphism invariant field theory for the dark sector, Phys. Rev. D **109**, 023537 (2024), arXiv:2311.16836 [astro-ph.CO].

[13] E. Alvarez, A. F. Faedo, and J. J. Lopez-Villarejo, Transverse gravity versus observations, JCAP **07**, 002, arXiv:0904.3298 [hep-th].

[14] E. Alvarez and A. F. Faedo, Unimodular cosmology and the weight of energy, Phys. Rev. D **76**, 064013 (2007), arXiv:hep-th/0702184.

[15] Y. Gouttenoire, G. Servant, and P. Simakachorn, Kination cosmology from scalar fields and gravitational-wave signatures, (2021), arXiv:2111.01150 [hep-ph].

[16] S. Dutta and R. J. Scherrer, Big Bang nucleosynthesis with a stiff fluid, Phys. Rev. D **82**, 083501 (2010), arXiv:1006.4166 [astro-ph.CO].

[17] O. Bertolami, P. Carrilho, and J. Paramos, Two-scalar-field model for the interaction of dark energy and dark matter, Phys. Rev. D **86**, 103522 (2012), arXiv:1206.2589 [gr-qc].

[18] K. J. Ludwick, The viability of phantom dark energy: A review, Mod. Phys. Lett. A **32**, 1730025 (2017), arXiv:1708.06981 [astro-ph.CO].

[19] N. Aghanim *et al.* (Planck), Planck 2018 results. VI. Cosmological parameters, Astron. Astrophys. **641**, A6 (2020), [Erratum: Astron.Astrophys. 652, C4 (2021)], arXiv:1807.06209 [astro-ph.CO].

[20] R. Amanullah *et al.*, Spectra and Light Curves of Six Type Ia Supernovae at $0.511 < z < 1.12$ and the Union2 Compilation, Astrophys. J. **716**, 712 (2010), arXiv:1004.1711 [astro-ph.CO].

[21] D. Jaramillo-Garrido, A. L. Maroto, and P. Martín-Moruno, Symmetry restoration for TDiff scalar fields, (2024), arXiv:2402.17422 [gr-qc].